The Journal of Immunology

Tupaia MAVS Is a Dual Target during Hepatitis C Virus Infection for Innate Immune Evasion and Viral Replication via NF- κB

Ling Xu, Dandan Yu, Yu-Lin Yao, Tianle Gu, Xiao Zheng, Yong Wu, Rong-Hua Luo, Yong-Tang Zheng, Jin Zhong and Yong-Gang Yao

J Immunol 2020; 205:2091-2099; Prepublished online 9 September 2020;
doi: 10.4049/jimmunol.2000376
http://www.jimmunol.org/content/205/8/2091

The Journal of Immunology is published twice each month by
The American Association of Immunologists, Inc.,
1451 Rockville Pike, Suite 650, Rockville, MD 20852

Print ISSN: 0022-1767 Online ISSN: 1550-6606.

Tupaia MAVS Is a Dual Target during Hepatitis C Virus Infection for Innate Immune Evasion and Viral Replication via NF-κB

Ling Xu,*,†,[1] Dandan Yu,*,†,[1] Yu-Lin Yao,*,†,‡ Tianle Gu,*,†,‡ Xiao Zheng,*,†,§ Yong Wu,*,† Rong-Hua Luo,*,† Yong-Tang Zheng,*,† Jin Zhong,¶ and Yong-Gang Yao*,†,‡,‖,#

Hepatitis C virus (HCV) infection is the cause of severe liver disease in many people. The restricted species tropism of HCV hinders the research and development of drugs and vaccines. The Chinese tree shrew (*Tupaia belangeri chinensis*) is a close relative of primates and can be infected by HCV, but the underlying mechanisms are unknown. In this study, we have characterized the functions of tree shrew MAVS (tMAVS) in response to HCV infection and defined the capacity of HCV replication. HCV was shown to be colocalized with tMAVS in primary tree shrew hepatocytes and cleaved tMAVS at site Cys508 via its NS3/4A protease, with a modulating effect by site Glu^{506} of tMAVS. The tMAVS cleavage by HCV NS3/4A impaired the IRF3-mediated induction of IFN-β but maintained the activated NF-κB signaling in the tree shrew primary cells. Activation of the tMAVS-dependent NF-κB signaling inversely inhibited HCV replication and might limit the establishment of persistent infection. Overall, our study has revealed an elegant example of the balance between the host defenses and HCV infection via the MAVS-mediated antiviral signaling and has provided an insight into the mechanisms underpinning HCV infection in the Chinese tree shrew. ***The Journal of Immunology*****, 2020, 205: 2091–2099.**

The hepatitis C virus (HCV) affects more than 71 million people worldwide, causing severe liver diseases, including chronically active hepatitis, cirrhosis, and hepatocellular carcinoma (1, 2). Current recommendations for treatment have a focus on the prevention of development of advanced liver diseases through the use of antiviral drugs. Although hundreds of medications for liver diseases caused by HCV have been developed (3), there are no effective vaccines available (4). The main problem is the lack of a permissive and immunocompetent animal model for HCV infection, despite the progress with the genetically humanized mouse model (5, 6). Besides the human, the chimpanzee is the only species that is naturally susceptible to HCV infection. However, the use of the chimpanzee as an HCV infection model is forbidden by ethical concerns and high cost (7). The tree shrew, which has a wide distribution in Southeast Asia and Southwest China (8) and a close genetic affinity to primates (9), has been used to create an HCV infection model (10). Early studies showed that tree shrew primary hepatocytes could be infected by HCV (11–13), and a high infection rate (>80%) was observed in the tree shrews challenged with patient- or cell culture–derived HCV (14). The tree shrew orthologs of vital HCV entry factors, such as CD81 (15), SR-BI (16), claudin-1, and occludin (17), supported HCV infection. However, infected animals frequently progressed to a low level of illness severity, with only a few animals developing severe liver disease after 3 y following the initial HCV infection (14). The underlying mechanism of HCV infection in this species needs to be explored further.

HCV has evolved a strategy to inhibit the early antiviral-signaling pathways that lead to the production of IFNs (18). The nonstructural NS3/4A complex of HCV is required for virus replication and can suppress the induction of the type I IFNs by cleaving the corresponding host factors (19). In the human, HCV NS3/4A specifically cleaves mitochondrial antiviral-signaling protein (MAVS)/IPS-1/VISA/Cardif (20–23) that is essential for antiviral innate immunity. In turn, MAVS released from the mitochondrial outer membrane allows HCV to escape from host immune surveillance (24). This viral innate immune evasion strategy may play a role in the transition of acute HCV infection to viral persistence in chronic infection (19). In simian primates, positive evolution of MAVS has led to resistance to the HCV

*Key Laboratory of Animal Models and Human Disease Mechanisms of the Chinese Academy of Sciences and Yunnan Province, Kunming Institute of Zoology, Chinese Academy of Sciences, Kunming, Yunnan 650223, China; †Kunming Institute of Zoology – Chinese University of Hong Kong Joint Laboratory of Bioresources and Molecular Research in Common Diseases, Kunming Institute of Zoology, Chinese Academy of Sciences, Kunming, Yunnan 650223, China; ‡Kunming College of Life Science, University of Chinese Academy of Sciences, Kunming, Yunnan 650204, China; §School of Life Sciences, Division of Life Sciences and Medicine, University of Science and Technology of China, Hefei, Anhui, 230026, China; ¶Key Laboratory of Molecular Virology and Immunology, Institute Pasteur of Shanghai, Chinese Academy of Sciences, Shanghai 200031, China; ‖National Resource Center for Non-Human Primates, Kunming Institute of Zoology, Chinese Academy of Sciences, Kunming, Yunnan 650107, China; and #National Research Facility for Phenotypic and Genetic Analysis of Model Animals (Primate Facility), Kunming Institute of Zoology, Chinese Academy of Sciences, Kunming, Yunnan 650107, China

[1]L.X. and D.Y. contributed equally to this work.

ORCIDs: 0000-0003-4769-935X (Y.W.); 0000-0001-5469-0324 (Y.-T.Z.); 0000-0002-3554-1275 (J.Z.); 0000-0002-2955-0693 (Y.-G.Y.).

Received for publication April 6, 2020. Accepted for publication August 7, 2020.

This work was supported by the National Natural Science Foundation of China (U1902215, U1402224, and 31700155), the Chinese Academy of Sciences "Light of West China" Program (xbzg-zdsys-201909), and the Applied Basic Research Foundation of Yunnan Province, Yunnan Department of Science and Technology (2016FB028 and 2018FB046).

Address correspondence and reprint requests to Dr. Yong-Gang Yao, Kunming Institute of Zoology, Chinese Academy of Sciences, Kunming 650223, Yunnan, China. E-mail address: yaoyg@mail.kiz.ac.cn

The online version of this article contains supplemental material.

Abbreviations used in this article: ACTB, β-actin; CAS, Chinese Academy of Sciences; HCV, hepatitis C virus; hMAVS, human MAVS; IFN-β–Luc, *IFNB1* promoter luciferase; KIZ, Kunming Institute of Zoology; MAVS, mitochondrial antiviral-signaling protein; MOI, multiplicity of infection; PTH, primary tree shrew hepatocyte; sgRNA, single-guide RNA; tMAVS, tree shrew MAVS; TSPRC, tree shrew primary renal cell; WT, wild type.

protease and resulted in escaping from hepaciviral antagonism (25). Whether HCV has evolved a similar strategy as in human to counteract the tree shrew immune system by targeting tree shrew MAVS (tMAVS) remains unanswered. Another unresolved question is whether the difference in the MAVS-mediated antiviral signaling between tree shrew and human could account for the different progress and development of severe liver diseases after HCV infection.

In this study, we have aimed to determine the functional conservation and diversification of MAVS and its downstream signaling in the Chinese tree shrew. We found that the HCV NS3/4A protease specifically cleaved tMAVS at the Cys^{508} residue, thus suppressing the IFN-β induction. HCV could only impair the IRF3-mediated induction of IFN-β while maintaining the activated NF-κB signaling. Activation of the NF-κB signaling was associated with restricted HCV replication.

Materials and Methods

Animals and ethics statement

The Chinese tree shrews (n = 10) were introduced from the experimental animal core facility of Kunming Institute of Zoology (KIZ), Chinese Academy of Sciences (CAS). After euthanasia, we collected liver and kidney tissues for preparation of primary cells. Animal experimental procedures and protocols were approved by the Institutional Animal Care and Use Committee of KIZ, CAS (approval no: SYDW20110315001) in accordance with the regulations in the Guide for the Care and Use of Laboratory Animals issued by the Ministry of Science and Technology of China.

Sequence alignment

MAVS mRNA sequences of nine mammalian species were retrieved from GenBank for comparison: *Homo sapiens* (human), NM_020746.4; *Macaca mulatta* (rhesus), NM_001042666.1; *Gorilla gorilla* (gorilla), XM_004061754.1; *Callithrix jacchus* (marmoset), XM_002747412.2; *Mus musculus* (mouse), NM_001206385.11; *Rattus norvegicus* (rat), NM_001005556.1; *Oryctolagus cuniculus* (rabbit), XM_002710888.1; *Pan troglodytes* (chimpanzee), XM_525410.2; and *Tupaia belangeri chinensis* (tree shrew), XP_006164034. Amino acid sequence alignment was performed using MUSCLE 3.7 (26) with the guidance of aligned protein sequences.

Abs

We used mouse monoclonal anti-Flag (M20008; Abmart), rabbit monoclonal anti-HA (M20008; Cell Signaling Technology), rabbit polyclonal anti-VISA (PRS4053; Sigma-Aldrich) to probe tMAVS, and rabbit polyclonal anti-MAVS (3993; Cell Signaling Technology) to probe human MAVS (hMAVS), respectively. The endogenous phospho–NF-κB, p65 (Ser^{536}), p65, phospho-IKKα/β ($Ser^{176/180}$), IKKα/β, phospho-IκBα (Ser^{32}), and IκBα were probed by using the NF-κB pathway sample kit (9936; Cell Signaling Technology). The other Abs used in this study included rabbit monoclonal anti-IRF3 (4302; Cell Signaling Technology), mouse monoclonal anti-HCV NS3 (ab13830; Abcam), mouse monoclonal anti-HCV core (MA1-080; Thermo Fisher Scientific), rabbit monoclonal anti-histone H3 (D1H2) (4499; Cell Signaling Technology), mouse monoclonal anti–β-actin (ACTB) (E1C602-2; EnoGene), mouse monoclonal anti-tubulin (Shanjin, ZA-0435), peroxidase-conjugated anti-mouse Ab (474-1806; KPL), and peroxidase-conjugated anti-rabbit Ab (074-1506; KPL).

Plasmid construction

The epitope-tagged tMAVS constructs and the tree shrew *IFNB1* promoter luciferase (IFN-β–Luc) reporter were described in our previous study (27). Coding region sequence of *hMAVS* using cDNA of 293T cells was cloned into Flag-tagged pCMV-3Tag-8 (240203; StrataGene). *tTRAF6*, *tTRAF3*, *tTBK1*, and *tIKKβ* were amplified using tree shrew spleen cDNA and were cloned into Flag-tagged pCMV-3Tag-8 with the indicated restriction endonuclease sites (Supplemental Table I). The cDNA encoding HCV NS3/4A was amplified from the HCV infectious clone (a kind gift from Dr. X. Chen of Wuhan Institute of Virology, CAS) and was cloned to pCMV-HA vector (631604; StrataGene) (Supplemental Table I). We generated expression vectors for hMAVS mutants (hMAVS C508R and V506E [hMAVS V506E]) and tMAVS mutants (tMAVS C508R and E506V [tMAVS E506V]) by using the multisite-directed mutagenesis (200518; StrataGene). All constructs were verified by sequencing.

Cell culture and virus infection

Huh7.5.1 (Huh-7–derived cell line) cells were introduced from Kunming Cell Bank, KIZ, CAS, and grown in DMEM (11965-092, BRL Model; Life Technologies) supplemented with 10% (vol/vol) FBS (10099-141, BRL Model; Life Technologies) and 1 × penicillin/streptomycin (10378016, BRL Model; Life Technologies) at 37˚C in 5% CO_2. Tree shrew primary renal cells (TSPRCs) and primary tree shrew hepatocytes (PTHs) were detached and cultured according to the enzyme-assisted dissection method as described previously (27–29). The HCV reporter virus (tagged by EGFP) (30) was a kind gift from X. Chen, Wuhan Institute of Virology, CAS, Yunnan, China. HCV was propagated in Huh7.5.1 cells, and the tissue culture ID_{50} of HCV was determined as described previously (29). PTHs were infected with HCV at a multiplicity of infection (MOI) of 10 at 37˚C for 6 h in primary liver-derived cell maintenance medium as described previously (29).

CRISPR/Cas9-mediated knockout of MAVS in cell lines

We used the CRISPR-Cas9 system (31) to knock out the *hMAVS* gene in Huh7.5.1 cells. The single-guide RNAs (sgRNAs) (Supplemental Table I) targeted the coding region as previously reported (32). The sgRNA pair was annealed and cloned into the pX330-T7 vector (a kind gift from Dr. P. Zheng, KIZ) expressing mCherry. The Huh7.5.1 cells were transfected with the pX330-T7 vector carrying the sgRNAs. Transfected cells expressing mCherry were sorted by flow cytometry and cultured for 48 h. Single cells were manually picked with a mouth pipette for expansion for around 3 wk. The AxyPrep Multisource Genomic DNA Miniprep Kit (26817KC1; Axygen) was used to extract genomic DNA of single Huh7.5.1 cells with potential knockout of hMAVS. The gene region spanning the sgRNA-targeting sites was amplified by using primer pair listed in Supplemental Table I. The PCR products were sequenced using the primer hMAVS–sgRNA–Fc to screen for mutation(s). We were able to pick up a cell clone with a frameshift mutation (c.583 insC) to disrupt the translation of hMAVS protein. We used the hMAVS polyclonal Ab to probe the endogenous hMAVS.

Luciferase reporter assay

TSPRCs were plated in 24-well plates at a density of 1×10^4 cells and cultured overnight. Cells were transfected with 0.1 μg of the luciferase reporter vectors IFN-β–Luc, NF-κB–Luc (pNF-κB–TA–Luc; 631912, Clontech Laboratories), or ISRE-Luc (ISRE *cis*-reporter; 219092, StrataGene), together with 0.01 μg pRL-SV40-*Renilla* (Promega; as an internal control), the indicated amounts of an empty vector (mock), or the indicated expression vector (Supplemental Table I) using X-tremeGENE HP DNA Transfection Reagent (06366546001; Roche Diagnostics). Cells were lysed and detected for luciferase activity by using the Dual-Luciferase Reporter Assay System (E1960; Promega) on Infinite M1000 PRO multimode microplate reader (30064852; Tecan). Results were shown as values normalized against each indicated MAVS overexpression without HCV NS3/4A (25).

Immunofluorescence analysis

Cells were fixed with 4% paraformaldehyde for 10 min and were incubated with the indicated respective primary Ab for MAVS (1:500), IRF3 (1:500), and p65 (1:500) overnight at 4˚C. The anti-Flag Ab (1:1000) or anti-HA Ab (1:1000) was used to detect the indicated proteins labeled by Flag or HA. After three washes with PBS (5 min each), immunoreactivity was detected by using the FITC-conjugated secondary Ab (1:500, 172-1506; KPL) for 1 h at room temperature. Nuclei were counterstained with 1 μg/ml DAPI (10236276001; Roche Diagnostics), and the slides were visualized under an Olympus FluoView 1000 confocal microscope (Olympus).

Western blotting

TSPRCs were grown in six-well plates at 70% confluence and were transfected with plasmids using X-tremeGENE HP DNA Transfection Reagent (06366546001; Roche). Cells were lysed on ice in radioimmunoprecipitation assay lysis buffer (P0013; Beyotime Institute of Biotechnology). Cytoplasm and nuclei were extracted from PTHs using the nuclear and cytoplasmic protein extraction kit (P0027-1; Beyotime Institute of Biotechnology) according to the manufacturer's instructions. Protein concentration was determined by using the BCA Protein Assay Kit (P0012; Beyotime Institute of Biotechnology). BSA (P0007; Beyotime Institute of Biotechnology) was used as a protein standard. Cell lysates

(25 μg total protein/sample) were separated by electrophoresis on 12% SDS-PAGE and transferred to polyvinylidene fluoride (PVDF) membranes (IPVH00010; Roche Diagnostics) using the standard procedures. The membranes were blocked with 5% (w/v) nonfat dry milk in TBST (TBS [no. 9997; Cell Signaling Technology]; Tween 20 [0.1%, P1379; Sigma-Aldrich]) at room temperature for 2 h. Membranes were incubated with primary Ab against VISA (1:1000), MAVS (1:1000), Flag (1:5000), IRF3 (1:1000), histone H3 (1:1000), tubulin (1:5000), phospho-p65 (1:1000), p65 (1:1000), phospho-IKKα/β (1:1000), IKKα/β (1:1000), phospho-IκBα (1:1000), and IκBα (1:1000), HCV NS3 (1:1000), HCV core (1:1000), and ACTB (1:10,000), respectively. Membranes were washed three times (5 min each) and were incubated for 1 h at room temperature with TBS containing 0.1% Tween 20–conjugated anti-mouse or anti-rabbit secondary Ab (1:10,000). After another round of three washes with TBST, the proteins on the membrane were detected by using ECL reagents (WBKLS0500; MilliporeSigma). ImageJ (National Institutes of Health, Bethesda, MD) was used to evaluate the relative densitometry. The p-p65, p-IKKα/β, and p-IκBα densitometric signal is determined by the ratio of p-p65, p-IKKα/β, p-IκBα to p65, IKKα/β, and IκBα, respectively, before normalized to ACTB or tubulin.

Statistical analysis

Comparisons between different groups were conducted by using the Student *t* test (Prism; GraphPad Software, CA). Data are presented as mean ± SD. A p value <0.05 was regarded as significantly different. All statistical analyses were two-tailed, with 95% confidence interval.

Results

HCV infection induces cellular redistribution of tMAVS

HCV NS3/4A can specifically target hMAVS for cleavage as part of its immune evasion strategy (23, 24). The NS3/4A cleavage resulted in subcellular redistribution of hMAVS, which was demonstrated both in cultured cell lines and in patients with HCV infection (24, 33). We previously characterized the MAVS ortholog from the Chinese tree shrew and demonstrated that tMAVS has an ability to suppress replication of various viruses (27). In this study, we have found that HCV infection causes the cleavage and redistribution of tMAVS: a faster migrating form (cleaved product) of tMAVS began to accumulate at 72 h and peaked at 96 h in PTHs infected with HCV (Fig. 1A). Moreover, we observed the redistribution of tMAVS from a typical mitochondrial network structure to a diffused cytosolic distribution (Fig. 1B). Along with the redistribution of tMAVS, we observed expression of the HCV NS3 protein in infected cells (Fig. 1A). This result indicated that the nonstructural proteins of HCV, presumably the NS3/4A protease, cleaved tMAVS. A clearly diffused cytosolic distribution of the cleaved tMAVS could also be found in TSPRCs that were overexpressed with HCV NS3/4A (Fig. 1C). Taken together, our results suggested that tMAVS redistribution was caused by the NS3/4A-mediated cleavage upon HCV infection.

HCV protease NS3/4A cleaves tMAVS at Cys^{508}

The HCV NS3/4A was known to specifically cleave hMAVS at residue Cys^{508} (23, 34), which is conserved in both human and tree shrew (Fig. 1D). We sought to determine whether HCV NS3/4A cleaved tMAVS at the same position. Consistent with the previous study (25), overexpression of hMAVS in TSPRCs was able to activate the IFN-β–Luc reporter, whereas coexpression of HCV NS3/4A significantly inhibited the hMAVS-mediated activation of the IFN-β–Luc (Fig. 1E, left). Similarly, overexpression of HCV NS3/4A inhibited the tMAVS-mediated signaling. This inhibition could be blocked by the change of Cys (C) to Arg (R) at the 508th position (C508R) in hMAVS and tMAVS (Fig. 1E). Both full-length and cleaved MAVS proteins were detected in cells coexpressing vectors HCV NS3/4A and MAVS. However, only the full-length form of the MAVS was detected in cells with ectopic expression of HCV NS3/4A and mutant MAVS C508R (Fig. 1E). The majority of tMAVS became cytosolic (presumably because of cleavage) when coexpressed with HCV NS3/4A (Fig. 1F). Note that overexpression of HCV NS3/4A had no apparent effect on mitochondrial structure (Supplemental Fig. 1A). Taken together, these results indicated that HCV NS3/4A could cleave tMAVS at Cys^{508}, in the same way as seen in hMAVS (23, 34).

The 506th residue of tMAVS does not protect it from HCV NS3/4A cleavage

Residue Val^{506} in hMAVS has been shown to be crucial for resistance to the HCV NS3/4A protease (25). Convergent evolution at the 506th residue in multiple primate species has resulted in an escape from antagonism by hepaciviruses, and changes at this residue have protected the MAVS from the cleavage by HCV NS3/4A protease (25). tMAVS has a Glu (E) instead of Val (V), as seen in human at the 506th position (Fig. 1D). According to the prediction of Patel et al. (25), residue Glu^{506} in tMAVS would protect it from the cleavage by HCV NS3/4A. However, we did not observe a significant protective effect in the presence of HCV NS3/4A, and tMAVS E506 (wild type [WT]) could be cleaved (Fig. 2A, right). When we swapped the Glu residue in tMAVS to the Val in human (tMAVS E506V) or replaced the Val residue in hMAVS with the Glu in tree shrew (hMAVS V506E), all these MVAS mutants could be cleaved by HCV NS3/4A, suggesting that the residue change (Val or Glu) at the 506th position in MAVS could not prevent the cleavage (Fig. 2A).

Intriguingly, we found that hMAVS WT was more susceptible to the HCV NS3/4A-mediated inhibition of the IFN-β–Luc than tMAVS WT (Fig. 2A). We hypothesized that different inhibitory effects of NS3/4A on the IFN-β–Luc might be caused by the residue Glu^{506} of tMAVS. Introducing residue Val^{506} in hMAVS into the tMAVS (tMAVS E506V) had a comparable inhibition effect relative to hMAVS WT in the presence of HCV NS3/4A (Fig. 2A). Consistent with this observation, mutant hMAVS V506E had a weaker inhibition effect on the induction of IFN-β–Luc reporter than hMAVS WT (Fig. 2A, left).

We further tested the NF-κB–Luc and ISRE-Luc reporter activities in TSPRCs overexpressing NS3/4A and MAVS or NS3/4A and MAVS mutant. We found that coexpression of tMAVS WT and HCV NS3/4A had a weaker inhibition effect on the activation of NF-κB–Luc reporter (Fig. 2B, right) compared with the coexpression of hMAVS WT and HCV NS3/4A (Fig. 2B, left), albeit a similar level of inhibition effect on the ISRE-Luc was observed (Fig. 2C). The tMAVS E506V showed a similar inhibitory effect on the ISRE-Luc reporter, comparing with tMAVS WT in the presence of HCV NS3/4A (Fig. 2C, right). However, mutant tMAVS E506V was more effective at blocking the induction of NF-κB–Luc reporter than tMAVS WT (Fig. 2B, right). Consistent with this observation, hMAVS V506E had a weaker inhibition effect on the induction of NF-κB–Luc reporter than hMAVS WT (Fig. 2B, left). All these results suggested that the Glu^{506} residue of the tMAVS modulated the inhibitory effect on the NF-κB signaling.

HCV infection induces the tMAVS-dependent NF-κB pathway activation

Type I IFN production requires the coordinated activation of a number of transcription factors, such as NF-κB and IRF3 (35). The activation of the NF-κB and IRF3 pathways were associated with the translocation of p65 and IRF3 from the cytoplasm into the nucleus, respectively. We examined the translocation of p65 and IRF3 in PTHs infected with HCV. Immunofluorescence assays of these cells showed that IRF3 remained in the cytoplasm after HCV

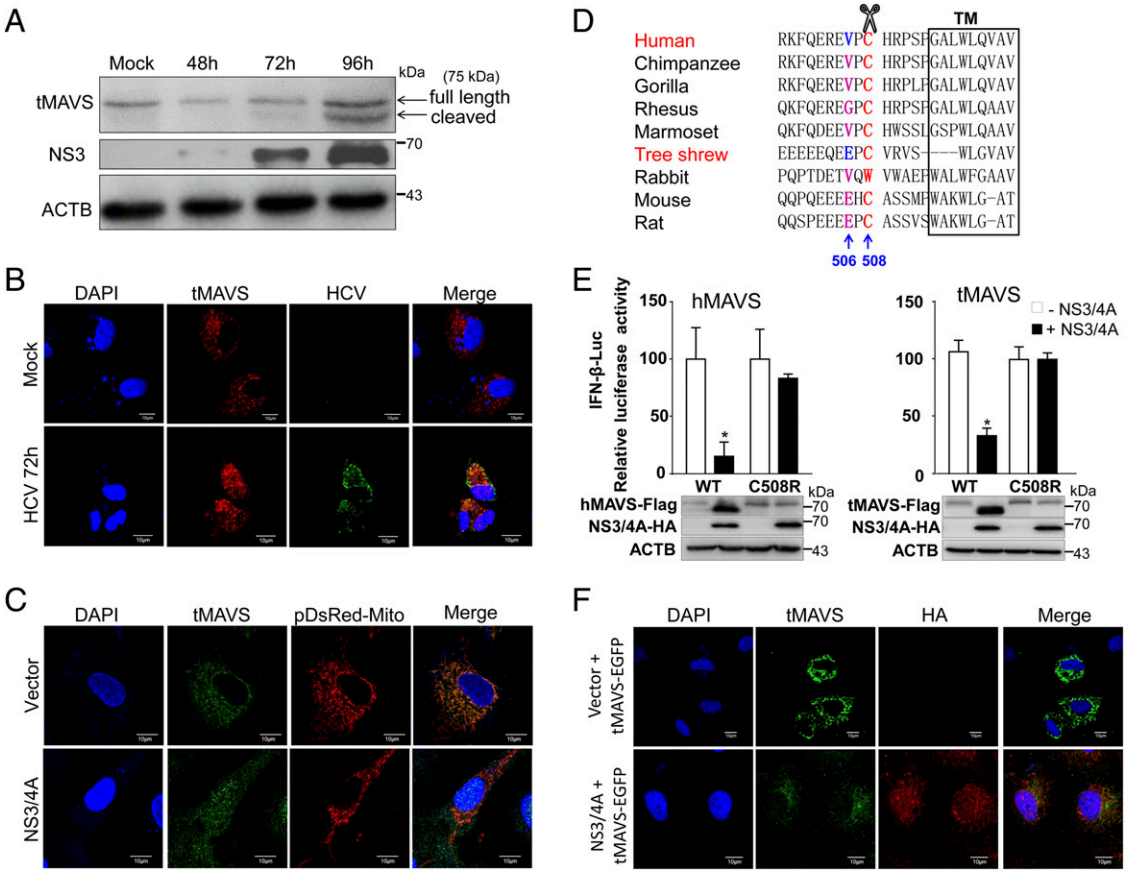

FIGURE 1. HCV cleaves tMAVS and jeopardizes the host antiviral response. (**A**) Cleavage of endogenous tMAVS protein during HCV infection. PTHs were harvested after HCV (JFH-1; MOI = 10) infection at the indicated times or without HCV infection (mock). Cell lysates were immunoblotted using the anti-VISA Ab and anti-HCV NS3 Ab, respectively. The ACTB was used as the loading control. (**B**) Expression of endogenous tMAVS (red) and HCV protein (HCV-GFP, green) in PTHs with (MOI = 10) or without HCV infection (mock) for 72 h. tMAVS was immunostained by using anti-VISA Ab to show the colocalization with HCV-GFP. Nuclei were stained with DAPI. (**C**) Change of endogenous tMAVS protein in the presence of HCV NS3/4A overexpression. TSPRCs were transfected with NS3/4A-HA vector or empty vector together with pDsRed-Mito for 48 h (concentration ratio 10:1). Endogenous tMAVS was immunostained to show the colocalization with mitochondria by using anti-VISA Ab. Nuclei were stained with DAPI. (**D**) Alignment of the MAVS transmembrane (TM) sequences of the Chinese tree shrew and other mammals retrieved from GenBank. The TM region predicted by the TMpred server (http://www.ch.embnet.org/software/TMPRED_form.html) is shown in box. Residues at the 506th and 508th sites are marked with different colors. (**E**) Activation of the IFN-β–Luc reporter in TSPRCs with overexpression of tMAVS and NS3/4A (+) or without NS3/4A (−). A change of Cys at the 508th position in the WT hMAVS to Arg (C508R) was used as the control for being unable to be cleaved by NS3/4A. TSPRCs were transfected with the IFN-β–Luc reporter vector (100 ng), TK (10 ng, as an inner control), and hMAVS-Flag or tMAVS-Flag expression vector (WT) or C508R (200 ng) for 24 h, then were transfected with empty vector (−NS3/4A; 200 ng) or NS3/4A-HA (+NS3/4A; 200 ng) for 12 h before the harvest for luciferase assay. Firefly luciferase activity was normalized as being 100% for overexpression of MAVS WT or C508R in the absence of NS3/4A. Immunoblot analyses showing MAVS, NS3/4A, and ACTB expression were listed in the below panel. Data shown are representative of three independent experiments. Bars represent means ± SD of three biological repeats in this representative. $*p < 0.05$, −NS3/4A versus +NS3/4A, Student *t* test. (**F**) Localization of tMAVS in the presence of NS3/4A. Expression vectors for Flag-NS3/4A and tMAVS-EGFP or empty vector were transfected into TSPRCs; Flag-NS3/4A was immunostained using Flag Ab. All data in (A)–(C) and (F) are representative of three independent experiments with similar results.

infection for 72 h, but p65 was translocated from the cytoplasm to the nucleus (Fig. 3A), and this nuclear translocation could be abolished by tMAVS knockdown (Fig. 3A, Supplemental Fig. 1B). Immunoblotting results showed that nuclear translocation of the p65 subunit of NF-κB was observed at 48 and 72 h after HCV infection, but there was no significant nuclear translocation of IRF3 (Fig. 3B). In addition, HCV infection significantly increased the mRNA levels of NF-κB–responsive genes (*MCP1* and *IL8*) at 72 h. tMAVS knockdown could abolish this increase (Fig. 3C) but had no effect on IRF3-responsive genes (*ISG15* and *ISG56*), suggesting that HCV infection could activate the NF-κB pathway in PTHs (12) in a tMAVS-dependent manner. Taken together, it was evident that the NF-κB signaling, but not the IRF3 pathway, was differentially maintained by HCV infection in a tMAVS-dependent manner.

The tMAVS residue Glu^{506} is involved in HCV-induced, tMAVS-dependent NF-κB signaling

To clarify whether tMAVS-mediated NF-κB pathway activation was dependent on the residue 506E of tMAVS, we studied the effect of tMAVS on NF-κB–Luc and ISRE-Luc reporter activations mediated by various effectors (Supplemental Fig. 1C) in the presence or absence of HCV NS3/4A in cotransfected TSPRCs. Cotransfection of tMAVS (WT or E506V) and each effector (tTRAF3, Fig. 4A; tTRAF6, Fig. 4B; tTBK1, Fig. 4C; or tIKKβ, Fig. 4D) remarkably activated ISRE-Luc and NF-κB–Luc reporter luciferase activities relative to transfection of tMAVS WT or E506V alone. Overexpression of NS3/4A significantly inhibited the induced ISRE-Luc reporter activated by cotransfection of tMAVS (WT or E506V) and the indicated effector (with the exception of

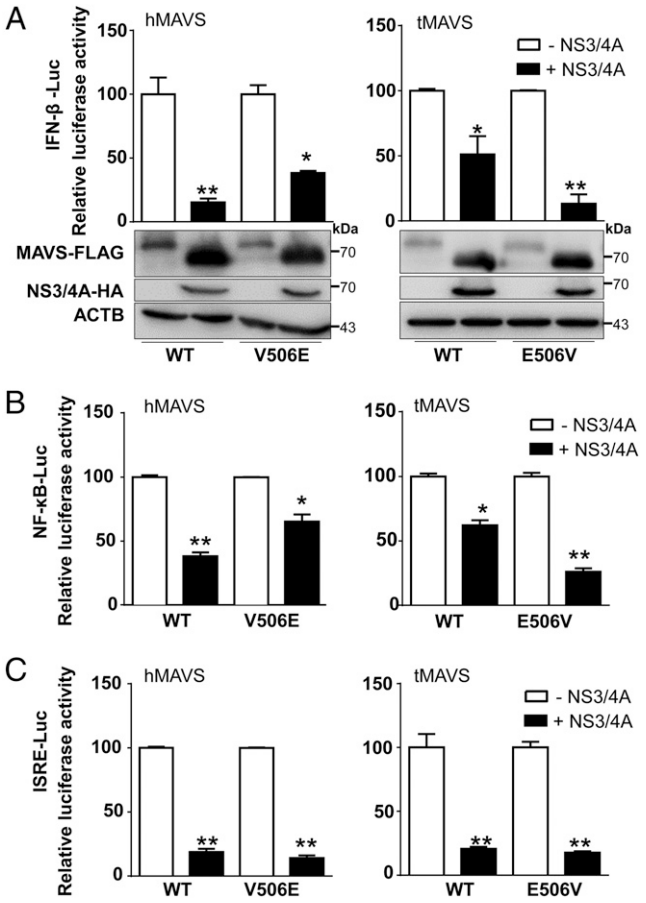

FIGURE 2. Residue Glu^{506} in tMAVS cannot protect it from being cleaved by HCV NS3/4A and has different effects on activating NF-κB–Luc reporters. The residues Glu^{506} (E506) and Val^{506} (V506) in MAVS had different effects on the activation of IFN-β–Luc reporter (**A**) and NF-κB–Luc reporter (**B**), but not ISRE-Luc reporter (**C**), in the presence of HCV NS3/4A protease, WT, hMAVS, or tMAVS. The experimental procedure and normalization of luciferase reporter activities are the same as Fig. 1E. Data are representative of three independent experiments with similar results. Bars represent means ± SD of three biological repeats in this representative. $*p < 0.05$, $**p < 0.01$, Student *t* test.

tIKKβ) (left column in each section of Fig. 4). However, no such inhibitory effect was observed on NF-κB–Luc reporter activation by NS3/4A in cells with cotransfection of tMAVS WT and each effector (upper, right column in each section of Fig. 4). In contrast, when we cotransfected tMAVS E506V and each effector, we observed a significant inhibition effect on NF-κB–Luc reporter activation by NS3/4A overexpression (below, right column in each section of Fig. 4). These results indicated that the residue 506E of tMAVS was involved in the tMAVS-dependent NF-κB pathway activation during HCV infection.

To investigate the potential role of residue Glu^{506} of tMAVS, we introduced the residue Glu into hMAVS and examined whether this mutant had any effect on HCV replication in Huh7.5.1 cells. Huh7.5.1 cells carry the T55I mutation in the first CARD of RIG-I, which disrupts the RIG-I–MAVS axis signaling pathway (36, 37). This cell line was thus more adaptable to imitate the tree shrew cells, which had a natural deficiency of RIG-I (38). We first generated hMAVS knockout Huh7.5.1 cells (named $Huh7.5.1^{MAVS-KO1}$) using the CRISPR-Cas9 technology (31). hMAVS knockout cell lines were generated by using the reported sgRNAs targeting exon 2 of hMAVS (32). Sequencing for genomic DNA and detection for endogenous hMAVS protein verified the complete knockout of hMAVS in the cell lines (Supplemental Fig. 1D, 1E). We then transfected the $Huh7.5.1^{MAVS-KO1}$ cells with hMAVS WT or hMAVS V506E and analyzed activation of the NF-κB signaling in response to HCV infection (Supplemental Fig. 1F). HCV infection decreased basal levels of phospho-p65 and phospho-IκBα in $Huh7.5.1^{MAVS-KO1}$ cells but had no apparent change of basal level of p-IKKα/β (Fig. 5A). Overexpression of hMAVS V506E remarkably activated the phospho-p65 and phospho-IKKα/β compared with hMAVS WT upon HCV infection at different titers (Fig. 5A). In contrast to hMAVS, overexpression of tMAVS WT in $Huh7.5.1^{MAVS-KO1}$ cells maintained better effect on the NF-κB signaling activation than tMAVS E506V (which has the human residue) in response to HCV infection (Fig. 5B). This result suggested that tMAVS with the human residue had an inferior role in the activation of the NF-κB signaling.

Change of the 506th residue in hMAVS is critical for HCV replication

Next, we infected the $Huh7.5.1^{MAVS-KO1}$ with HCV (MOI = 0.5) and transfected with expression vectors hMAVS WT, hMAVS V506E, and hMAVS C508R, respectively. The hMAVS C508R was used as a positive control, according to the previous report (39), to show the robustness of our cellular system. The HCV RNA levels were determined by quantitative real-time PCR to indicate the viral replication. We found that HCV RNA was decreased in the $Huh7.5.1^{MAVS-KO1}$ cells with overexpression of hMAVS C508R, which was likely caused by the resistance to cleavage by HCV NS3/4A, so that the antiviral effect of the induced IFNs was maintained (Fig. 6A). The HCV RNA replication was significantly reduced in cells overexpressing hMAVS V506E compared with hMAVS WT (Fig. 6A, upper). Consistently, hMAVS V506E, but not hMAVS WT, decreased core protein level in $Huh7.5.1^{MAVS-KO1}$ cells during HCV infection (Figs. 5A, 6A). These results suggested that the 506th residue in hMAVS was critical for HCV replication, and residue 506E was required for restricting HCV replication.

To verify whether the NF-κB signaling mediated by the 506th residue in MAVS was associated with HCV replication, we examined the activation effect of the NF-κB signaling by using chemicals (VP16, activator of the NF-κB signaling (40); BAY, an NF-κB inhibitor, inhibits IκBα phosphorylation) in $Huh7.5.1^{MAVS-KO1}$ cells transfected with expression vectors for hMAVS WT and hMAVS V506E, respectively. We consistently produced the activation and inhibition of the NF-κB signaling in $Huh7.5.1^{MAVS-KO1}$ cells by treatment with VP16 and BAY, respectively (Supplemental Fig. 1G). Compared with the control cells (cells treated with DMSO), treatment of VP16 reduced the level of HCV core protein in cells overexpressing hMAVS WT or hMAVS V506E, whereas treatment of BAY significantly increased HCV core protein expression (Fig. 6B). A similar pattern was observed for $Huh7.5.1^{MAVS-KO1}$ cells with overexpression of tMAVS WT or tMAVS E506V treated with or without VP16 and BAY (Fig. 6C). Note that VP16 and BAY might have broad effects on unspecific targets, and the conclusion of NF-κB–specific regulation on HCV replication by using these chemical treatments should be received with caution.

Relative to cells overexpressing hMAVS WT, cells overexpressing hMAVS V506E showed a reduced level of HCV core protein in each comparison with the same chemical treatment (DMSO and BAY), suggesting that hMAVS V506E had an enhanced inhibition effect on HCV replication compared with hMAVS WT (Fig. 6B). Conversely, tMAVS E506V had an inferior inhibition effect on HCV replication relative to tMAVS WT

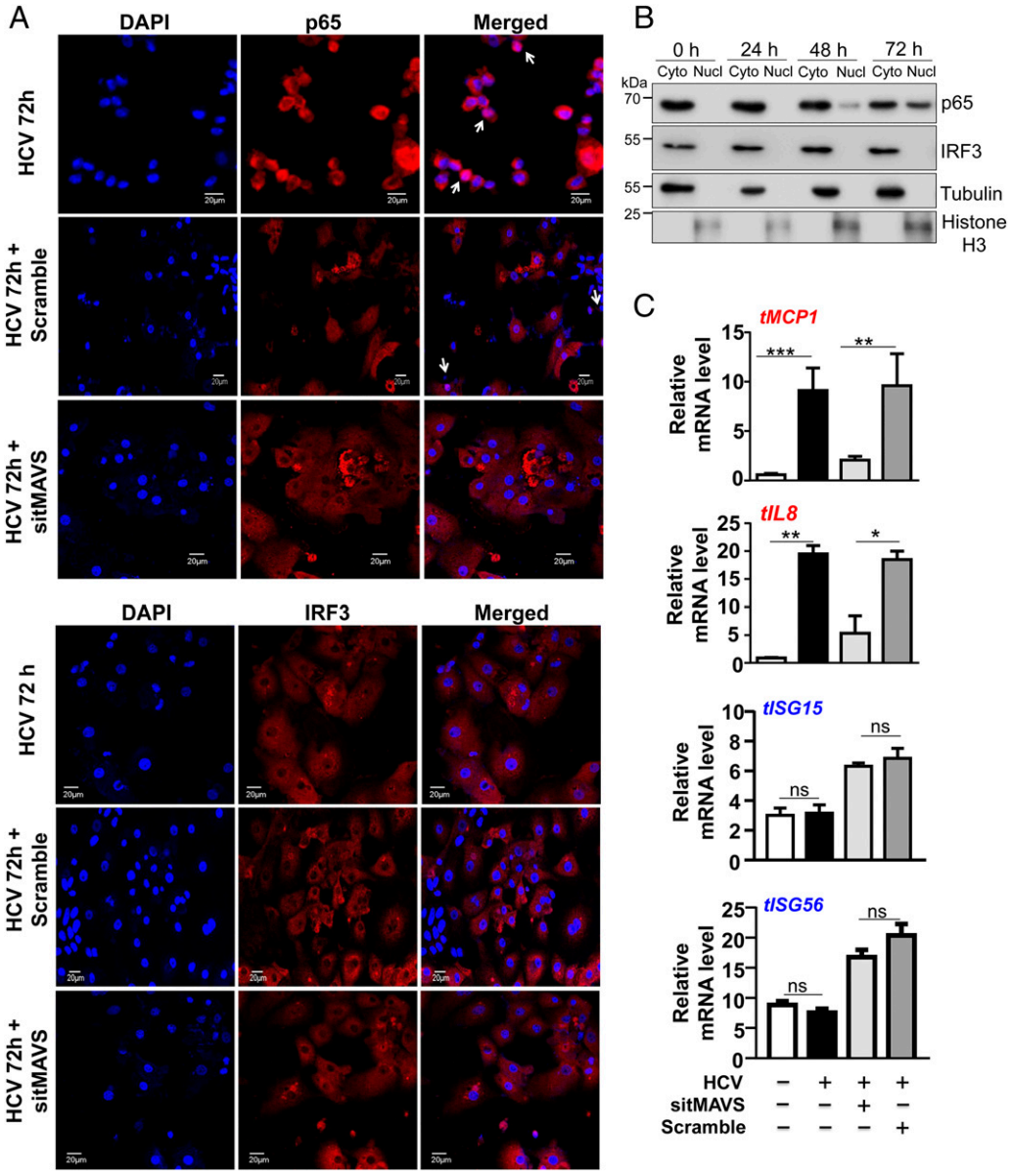

FIGURE 3. HCV inhibits tMAVS-induced IRF3 activation, but has no inhibitory effect on NF-κB signaling. (**A**) Activation of endogenous NF-κB p65 and IRF3 proteins in HCV-infected PTHs with or without tMAVS knockdown. PTHs were infected with HCV (MOI = 10) for 24 h and were transfected with the small-interring RNA (siRNA) negative control (scramble, 50 nM) or siRNA for tMAVS (sitMAVS; 50 nM) for 48 h. The endogenous NF-κB p65 and IRF3 proteins were immunostained by using anti–NF-κB p65 Ab and anti-IRF3 Ab, respectively. Nuclei were stained with DAPI. (**B**) Nuclear translocation of endogenous NF-κB p65 and IRF3 proteins during HCV infection in PTHs. Cells (1×10^7) were infected with HCV-GFP (MOI = 10) and were collected at the indicated time points. Cytoplasm (Cyto) and nuclei (Nucl) were extracted and analyzed for the protein levels of NF-κB p65 and IRF3 by using anti–NF-κB p65 Ab and anti-IRF3 Ab, respectively. Endogenous tubulin and histone H3 were used as cytoplasmic and nuclear markers, respectively. (**C**) Knockdown of tMAVS inhibits HCV-induced upregulation of the NF-κB–responsive genes. The PTHs (1×10^6) were infected with HCV (MOI = 10) or uninfected for 24 h, then transfected with the siRNA negative control (scramble, 50 nM) or sitMAVS (50 nM) for 48 h. The mRNA levels of *tMCP1*, *tIL8*, *tISG15*, and *tISG56* were measured by quantitative real-time PCR (RT-qPCR), with normalization to *ACTB*. All data in (A)–(C) are representative of three independent experiments with similar results. Bars in (C) represent means ± SD of three biological repeats in the representative. $^*p < 0.05$, $^{**}p < 0.01$, $^{***}p < 0.001$, Student *t* test. ns, not significant.

(Fig. 6C). These results further supported that the residue 506E in MAVS was involved in the MAVS-mediated NF-κB activation to inhibit HCV replication.

Discussion

There is a shortage of animal models for HCV study because of the selective HCV susceptibility seen only in humans and chimpanzees (7, 41). Most simian orthologs of HCV entry factors share a high degree of sequence identity with those of humans and chimpanzees (41), but these animals are not susceptible to HCV infection. The barriers to HCV transmission across different species are poorly defined. Also, the viral innate immune evasion strategies and human genetic determinants might underlie the transition of acute HCV infection to viral persistence during chronic infection (19).

As a central component of the innate immune evasion, HCV NS3/4A cleaved MAVS from mitochondria or mitochondrial-associated membranes to attenuate IFN production (23, 33, 37, 42). Cleavage of MAVS has been detected in the liver of patients with chronic HCV infection (33, 43) and caused a low

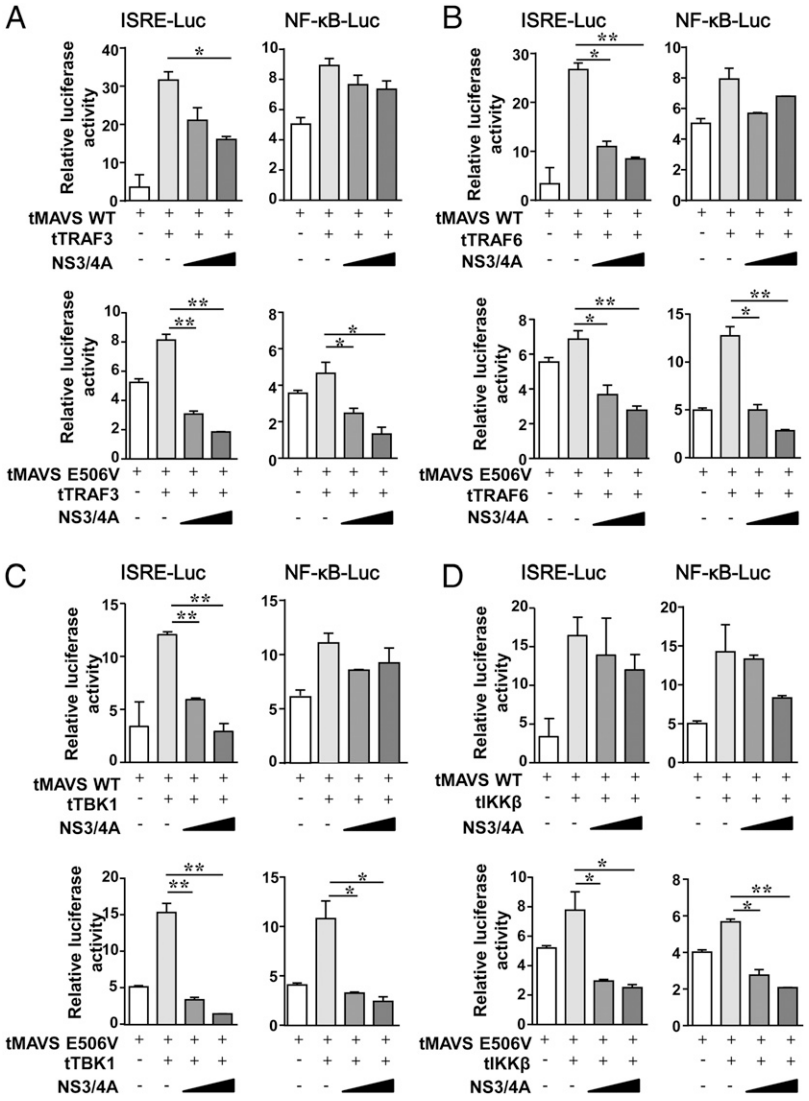

FIGURE 4. HCV NS3/4A inhibits tMAVS-induced IRF3 signaling, but not NF-κB pathway. TSPRCs were transfected with the indicated luciferase vector (100 ng), expression vector of tTRAF3 (**A**), tTRAF6 (**B**), tTBK1 (**C**), or tIKKβ (**D**) (100 ng), together with tMAVS WT (upper) or tMAVS E506V (lower) vector (100 ng) for 24 h, then were transfected with empty vector (−NS3/4A; 200 ng) or with increased amount of NS3/4A-HA (+NS3/4A; 100 or 200 ng, with empty vector to reach a total amount of 200 ng) for 24 h before the luciferase analysis. Overexpression of tMAVS WT or E506V, together with each indicated effector (tTRAF3, tTRAF6, tTBK1, or tIKKβ), was used as the control for evaluating the inhibitory effect by NS3/4A. All data are representative of three independent experiments with similar results. Bars represent means ± SD of three biological repeats in the representative. $*p < 0.05$, $**p < 0.01$, Student t test.

level of the IFN pathway activation (43). Given the importance of MAVS during HCV infection, we speculated that the tree shrew possesses susceptible MAVS that could allow for laboratory-introduced HCV infection in this species. Similar to that of human, we found that tMAVS served as the proteolytic target of HCV NS3/4A protease. Specifically, HCV cleaved tMAVS at residue Cys^{508}, released MAVS from the mitochondria, and prevented the induction of IFN-β. These results provided functional evidence for an active role of tMAVS to support HCV infection.

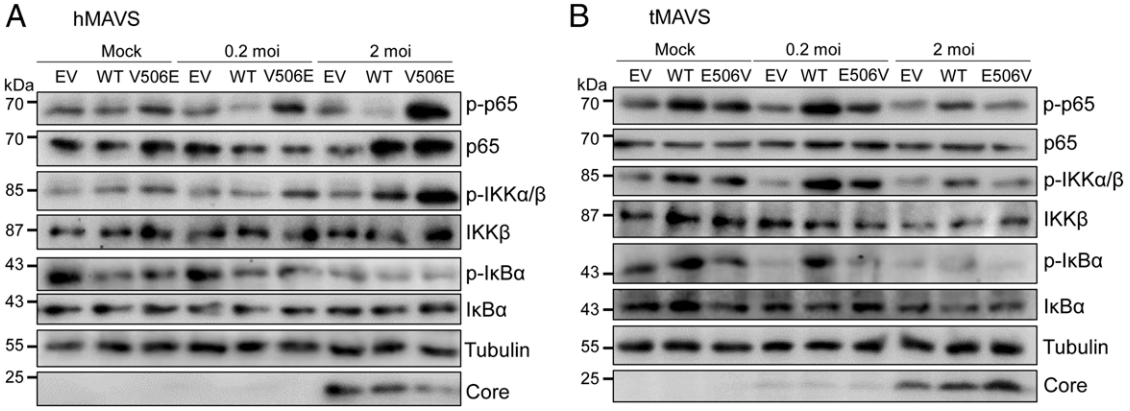

FIGURE 5. MAVS Glu^{506} affects the NF-κB signaling pathway. Huh7.5.1$^{MAVS\text{-}KO1}$ cells (4×10^5) were infected with HCV (MOI = 0.2 or 2) or uninfected (mock) for 72 h, then were transfected with (**A**) empty vector (EV) and expression vectors for hMAVS WT, hMAVS V506E, or (**B**) EV, tMAVS WT, or tMAVS E506V (2.5 μg each) for 48 h, respectively. Cell lysates were immunoblotted using the NF-κB signaling pathway sample kit. Shown are representative of three independent experiments, with similar results.

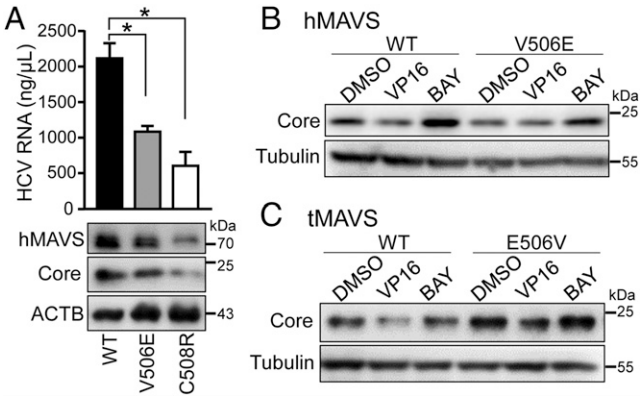

FIGURE 6. Change of the 506th residue affects HCV replication. (**A**) Change of the 506th residue affects HCV RNA copy number (upper) and core protein expression (below). Huh7.5.1$^{MAVS\text{-}KO1}$ cells were infected with HCV (MOI = 0.5) for 72 h, then were transfected with expression vectors hMAVS WT, hMAVS V506E, and hMAVS C508R. Cells were harvested at 48 h after transfection for quantitative real-time PCR (RT-qPCR) assay to determine HCV RNA (upper) and for immunoblot by using the anti-MAVS Ab and anti-HCV core Ab, respectively. The ACTB was used as the loading control (below). (**B** and **C**) Suppression of the NF-κB signaling promotes HCV infection in the Huh7.5.1$^{MAVS\text{-}KO1}$ cells overexpressing hMAVS WT or hMAVS V506E (B), tMAVS WT, or tMAVS E506V (C). The Huh7.5.1$^{MAVS\text{-}KO1}$ cells (1×10^6) were infected with HCV (MOI = 2) for 72 h and were transfected with expression vector hMAVS WT, hMAVS V506E, tMAVS WT, or tMAVS E506V (2.5 μg each) for 12 h, respectively. Cells were treated with vehicle (DMSO), BAY11 (10 μM), or VP16 (10 μM) for 48 h before the harvest for the immunoblot assay. All Western blot data are representative of three independent experiments with similar results. For HCV RNA copy number quantification, this assay was independently repeated at least three times with similar results, and the representative one was shown as bars (means ± SD of three biological repeats in the representative assay). *$p < 0.05$, Student *t* test.

The 506th residue of MAVS in primates has evolved under strong positive selection and has changed repeatedly during evolution to account for HCV antagonism (25). This is the possible reason why primates possessing MAVS resistant to NS3/4A cleavage (residue 506 is not Val) should be better at clearing hepaciviral infections than species with susceptible MAVS (Val^{506}) (25). tMAVS has Glu at the 506th residue but is susceptible to cleavage. Similarly, murine MAVS also has a Glu instead of Val at the 506th residue (Fig. 1D) and can be cleaved by HCV NS3/4A according to the study of Nandakumar et al. (44). These results seemed to suggest that residue Val^{506} in MAVS was not the only residue essential for the HCV NS/4A cleavage. There was no positive selection at the 506th residue of the tMAVS and murine MAVS (data not shown), which was different from that of primates as reported by Patel et al. (25). The exact mechanism underlying the cleavage at the 506th position remained to be elucidated. It would be rewarding to test whether the cleaved portion of MAVS bound to some unknown partners in the affected signaling. Note that HCV inhibition effect on tMAVS and NF-κB signaling seemed to be NS3/4A specific, as other HCV proteins, including core, NS4B, NS5A, and NS5B, had no such inhibitory effect (data not shown).

HCV NS3/4A could prevent the hMAVS-mediated activation of NF-κB and IRF3 signaling (23, 37). We found that hMAVS was more sensitive to the cleavage effect of NS3/4A on the inhibition of IFN-β–Luc and NF-κB–Luc activities than tMAVS, which might be caused by different residues at the 506th site in human and tree shrew. Indeed, our assays for hMAVS with the tree shrew residue Glu^{506} showed that hMAVS V506E behaved like tMAVS in response to HCV infection for activation of the NF-κB and IFN signaling. In addition, we found that HCV inhibited the tMAVS–IRF3, but not the tMAVS–NF-κB, signaling in tree shrew cells. Therefore, HCV might be capable of antagonizing the tMAVS–IRF3 signaling while the activation of the NF-κB signaling in tree shrew is maintained.

Although our current results have indicated that HCV uses a similar way as seen in human to escape the innate immune response in tree shrew, we found that HCV NS3/4A impairs the IRF3-mediated induction of IFN-β, but this is balanced by the activation of NF-κB signaling, which restricts HCV replication and affects the immune response to the invading pathogen. Our findings have suggested that tMAVS could serve as a double-edged sword for HCV targeting in the tree shrew and have provided new insights into the mechanisms underpinning HCV infection in this animal and the creation of HCV infection animal models.

Acknowledgments

We thank Dr. Ian Logan for language editing and helpful comments on the early version of this manuscript. We are also grateful to the two anonymous reviewers for critical comments.

Disclosures

The authors have no financial conflicts of interest.

References

1. Mohd Hanafiah, K., J. Groeger, A. D. Flaxman, and S. T. Wiersma. 2013. Global epidemiology of hepatitis C virus infection: new estimates of age-specific antibody to HCV seroprevalence. *Hepatology* 57: 1333–1342.
2. Maasoumy, B., and H. Wedemeyer. 2012. Natural history of acute and chronic hepatitis C. *Best Pract. Res. Clin. Gastroenterol.* 26: 401–412.
3. El Khoury, A. C., W. K. Klimack, C. Wallace, and H. Razavi. 2012. Economic burden of hepatitis C-associated diseases in the United States. *J. Viral Hepat.* 19: 153–160.
4. Wang, X., Y. Yan, T. Gan, X. Yang, D. Li, D. Zhou, Q. Sun, Z. Huang, and J. Zhong. 2019. A trivalent HCV vaccine elicits broad and synergistic polyclonal antibody response in mice and rhesus monkey. *Gut* 68: 140–149.
5. Dorner, M., J. A. Horwitz, J. B. Robbins, W. T. Barry, Q. Feng, K. Mu, C. T. Jones, J. W. Schoggins, M. T. Catanese, D. R. Burton, et al. 2011. A genetically humanized mouse model for hepatitis C virus infection. *Nature* 474: 208–211.
6. Dorner, M., J. A. Horwitz, B. M. Donovan, R. N. Labitt, W. C. Budell, T. Friling, A. Vogt, M. T. Catanese, T. Satoh, T. Kawai, et al. 2013. Completion of the entire hepatitis C virus life cycle in genetically humanized mice. *Nature* 501: 237–241.
7. Lanford, R. E., C. M. Walker, and S. M. Lemon. 2017. The chimpanzee model of viral hepatitis: advances in understanding the immune response and treatment of viral hepatitis. *ILAR J.* 58: 172–189.
8. Peng, Y. Z., Z. Z. Ye, R. J. Zou, Y. X. Wang, B. P. Tian, Y. Y. Ma, and L. M. Shi. 1991. *Biology of Chinese Tree Shrews (Tupaia belangeri chinensis).* Yunnan Science and Technology Press, Kunming, China.
9. Fan, Y., M.-S. Ye, J.-Y. Zhang, L. Xu, D.-D. Yu, T.-L. Gu, Y.-L. Yao, J.-Q. Chen, L.-B. Lv, P. Zheng, et al. 2019. Chromosomal level assembly and population sequencing of the Chinese tree shrew genome. *Zool. Res.* 40: 506–521.
10. Zheng, Y.-T., Y.-G. Yao, and L. Xu. 2014. *Basic Biology and Disease Models of Chinese Tree Shrews.* Yunnan Science and Technology Press, Kunming, China, p. 391–393.
11. Barth, H., R. Cerino, M. Arcuri, M. Hoffmann, P. Schürmann, M. I. Adah, B. Gissler, X. Zhao, V. Ghisetti, B. Lavezzo, et al. 2005. Scavenger receptor class B type I and hepatitis C virus infection of primary tupaia hepatocytes. *J. Virol.* 79: 5774–5785.
12. Guitart, A., J. I. Riezu-Boj, E. Elizalde, E. Larrea, C. Berasain, R. Aldabe, M. P. Civeira, and J. Prieto. 2005. Hepatitis C virus infection of primary tupaia hepatocytes leads to selection of quasispecies variants, induction of interferon-stimulated genes and NF-kappaB nuclear translocation. *J. Gen. Virol.* 86: 3065–3074.
13. Xu, X., H. Chen, X. Cao, and K. Ben. 2007. Efficient infection of tree shrew (*Tupaia belangeri*) with hepatitis C virus grown in cell culture or from patient plasma. *J. Gen. Virol.* 88: 2504–2512.
14. Amako, Y., K. Tsukiyama-Kohara, A. Katsume, Y. Hirata, S. Sekiguchi, Y. Tobita, Y. Hayashi, T. Hishima, N. Funata, H. Yonekawa, and M. Kohara. 2010. Pathogenesis of hepatitis C virus infection in *Tupaia belangeri*. *J. Virol.* 84: 303–311.
15. Tian, Z. F., H. Shen, X. H. Fu, Y. C. Chen, H. E. Blum, T. F. Baumert, and X. P. Zhao. 2009. Interaction of hepatitis C virus envelope glycoprotein E2 with the large extracellular loop of *tupaia* CD81. *World J. Gastroenterol.* 15: 240–244.

16. Jia, Z. S., D. W. Du, Y. F. Lei, X. Wei, W. Yin, L. Ma, J. Q. Lian, P. Z. Wang, D. Li, and Y. X. Zhou. 2008. Scavenger receptor class B type I mediates cell entry of hepatitis C virus. *J. Int. Med. Res.* 36: 1319–1325.
17. Tong, Y., Y. Zhu, X. Xia, Y. Liu, Y. Feng, X. Hua, Z. Chen, H. Ding, L. Gao, Y. Wang, et al. 2011. Tupaia CD81, SR-BI, claudin-1, and occludin support hepatitis C virus infection. *J. Virol.* 85: 2793–2802.
18. Park, S. H., and B. Rehermann. 2014. Immune responses to HCV and other hepatitis viruses. *Immunity* 40: 13–24.
19. Horner, S. M., and M. Gale, Jr. 2013. Regulation of hepatic innate immunity by hepatitis C virus. *Nat. Med.* 19: 879–888.
20. Kawai, T., K. Takahashi, S. Sato, C. Coban, H. Kumar, H. Kato, K. J. Ishii, O. Takeuchi, and S. Akira. 2005. IPS-1, an adaptor triggering RIG-I- and Mda5-mediated type I interferon induction. *Nat. Immunol.* 6: 981–988.
21. Seth, R. B., L. Sun, C. K. Ea, and Z. J. Chen. 2005. Identification and characterization of MAVS, a mitochondrial antiviral signaling protein that activates NF-kappaB and IRF 3. *Cell* 122: 669–682.
22. Xu, L. G., Y. Y. Wang, K. J. Han, L. Y. Li, Z. Zhai, and H. B. Shu. 2005. VISA is an adapter protein required for virus-triggered IFN-beta signaling. *Mol. Cell* 19: 727–740.
23. Meylan, E., J. Curran, K. Hofmann, D. Moradpour, M. Binder, R. Bartenschlager, and J. Tschopp. 2005. Cardif is an adaptor protein in the RIG-I antiviral pathway and is targeted by hepatitis C virus. *Nature* 437: 1167–1172.
24. Lin, R., J. Lacoste, P. Nakhaei, Q. Sun, L. Yang, S. Paz, P. Wilkinson, I. Julkunen, D. Vitour, E. Meurs, and J. Hiscott. 2006. Dissociation of a MAVS/IPS-1/VISA/Cardif-IKKepsilon molecular complex from the mitochondrial outer membrane by hepatitis C virus NS3-4A proteolytic cleavage. *J. Virol.* 80: 6072–6083.
25. Patel, M. R., Y.-M. Loo, S. M. Horner, M. Gale, Jr., and H. S. Malik. 2012. Convergent evolution of escape from hepaciviral antagonism in primates. *PLoS Biol.* 10: e1001282.
26. Edgar, R. C. 2004. MUSCLE: multiple sequence alignment with high accuracy and high throughput. *Nucleic Acids Res.* 32: 1792–1797.
27. Xu, L., D. Yu, L. Peng, Y. Fan, J. Chen, Y. T. Zheng, C. Wang, and Y. G. Yao. 2015. Characterization of a MAVS ortholog from the Chinese tree shrew (*Tupaia belangeri chinensis*). *Dev. Comp. Immunol.* 52: 58–68.
28. Xu, L., D. Yu, L. Peng, Y. Wu, Y. Fan, T. Gu, Y.-L. Yao, J. Zhong, X. Chen, and Y.-G. Yao. 2020. An alternative splicing of Tupaia STING modulated anti-RNA virus responses by targeting MDA5-LGP2 and IRF3. *J. Immunol*. 204: 3191–3204.
29. Yu, D., Y. Wu, L. Xu, Y. Fan, L. Peng, M. Xu, and Y. G. Yao. 2016. Identification and characterization of toll-like receptors (TLRs) in the Chinese tree shrew (*Tupaia belangeri chinensis*). *Dev. Comp. Immunol.* 60: 127–138.
30. Han, Q., C. Xu, C. Wu, W. Zhu, R. Yang, and X. Chen. 2009. Compensatory mutations in NS3 and NS5A proteins enhance the virus production capability of hepatitis C reporter virus. *Virus Res.* 145: 63–73.
31. Ran, F. A., P. D. Hsu, J. Wright, V. Agarwala, D. A. Scott, and F. Zhang. 2013. Genome engineering using the CRISPR-Cas9 system. *Nat. Protoc.* 8: 2281–2308.
32. Sun, X., L. Sun, Y. Zhao, Y. Li, W. Lin, D. Chen, and Q. Sun. 2016. MAVS maintains mitochondrial homeostasis via autophagy. *Cell Discov.* 2: 16024.
33. Loo, Y. M., D. M. Owen, K. Li, A. K. Erickson, C. L. Johnson, P. M. Fish, D. S. Carney, T. Wang, H. Ishida, M. Yoneyama, et al. 2006. Viral and therapeutic control of IFN-beta promoter stimulator 1 during hepatitis C virus infection. *Proc. Natl. Acad. Sci. USA* 103: 6001–6006.
34. Li, X. D., L. Sun, R. B. Seth, G. Pineda, and Z. J. Chen. 2005. Hepatitis C virus protease NS3/4A cleaves mitochondrial antiviral signaling protein off the mitochondria to evade innate immunity. *Proc. Natl. Acad. Sci. USA* 102: 17717–17722.
35. Tamura, T., H. Yanai, D. Savitsky, and T. Taniguchi. 2008. The IRF family transcription factors in immunity and oncogenesis. *Annu. Rev. Immunol.* 26: 535–584.
36. Zhong, J., P. Gastaminza, G. Cheng, S. Kapadia, T. Kato, D. R. Burton, S. F. Wieland, S. L. Uprichard, T. Wakita, and F. V. Chisari. 2005. Robust hepatitis C virus infection *in vitro*. *Proc. Natl. Acad. Sci. USA* 102: 9294–9299.
37. Foy, E., K. Li, R. Sumpter, Jr., Y. M. Loo, C. L. Johnson, C. Wang, P. M. Fish, M. Yoneyama, T. Fujita, S. M. Lemon, and M. Gale, Jr. 2005. Control of antiviral defenses through hepatitis C virus disruption of retinoic acid-inducible gene-I signaling. *Proc. Natl. Acad. Sci. USA* 102: 2986–2991.
38. Xu, L., D. Yu, Y. Fan, L. Peng, Y. Wu, and Y.-G. Yao. 2016. Loss of RIG-I leads to a functional replacement with MDA5 in the Chinese tree shrew. *Proc. Natl. Acad. Sci. USA* 113: 10950–10955.
39. Cao, X., Q. Ding, J. Lu, W. Tao, B. Huang, Y. Zhao, J. Niu, Y.-J. Liu, and J. Zhong. 2015. MDA5 plays a critical role in interferon response during hepatitis C virus infection. *J. Hepatol.* 62: 771–778.
40. Wu, Z. H., and S. Miyamoto. 2008. Induction of a pro-apoptotic ATM-NF-kappaB pathway and its repression by ATR in response to replication stress. *EMBO J.* 27: 1963–1973.
41. Burm, R., L. Collignon, A. A. Mesalam, and P. Meuleman. 2018. Animal models to study hepatitis C virus infection. *Front. Immunol.* 9: 1032.
42. Baril, M., M. E. Racine, F. Penin, and D. Lamarre. 2009. MAVS dimer is a crucial signaling component of innate immunity and the target of hepatitis C virus NS3/4A protease. *J. Virol.* 83: 1299–1311.
43. Bellecave, P., M. Sarasin-Filipowicz, O. Donzé, A. Kennel, J. Gouttenoire, E. Meylan, L. Terracciano, J. Tschopp, C. Sarrazin, T. Berg, et al. 2010. Cleavage of mitochondrial antiviral signaling protein in the liver of patients with chronic hepatitis C correlates with a reduced activation of the endogenous interferon system. *Hepatology* 51: 1127–1136.
44. Nandakumar, R., K. Finsterbusch, C. Lipps, B. Neumann, M. Grashoff, S. Nair, I. Hochnadel, S. Lienenklaus, I. Wappler, E. Steinmann, et al. 2013. Hepatitis C virus replication in mouse cells is restricted by IFN-dependent and -independent mechanisms. *Gastroenterology* 145: 1414–1423.e1.

Published January 13, 2021, doi:10.4049/jimmunol.2001396

Corrections

Xu, L., D. Yu, Y.-L. Yao, T. Gu, X. Zheng, Y. Wu, R.-H. Luo, Y.-T. Zheng, J. Zhong, and Y.-G. Yao. 2020. *Tupaia* MAVS is a dual target during hepatitis C virus infection for innate immune evasion and viral replication via NF-κB. *J. Immunol.* 205: 2091–2099.

In Fig. 5, the molecular mass for tubulin was incorrect as originally published. The correct molecular mass is 55 kDa. The corrected version of Fig. 5 is shown below. The figure legend was correct as published and is shown below for reference. Fig. 5 has been corrected in the online version of the article, which now differs from the print version as originally published.

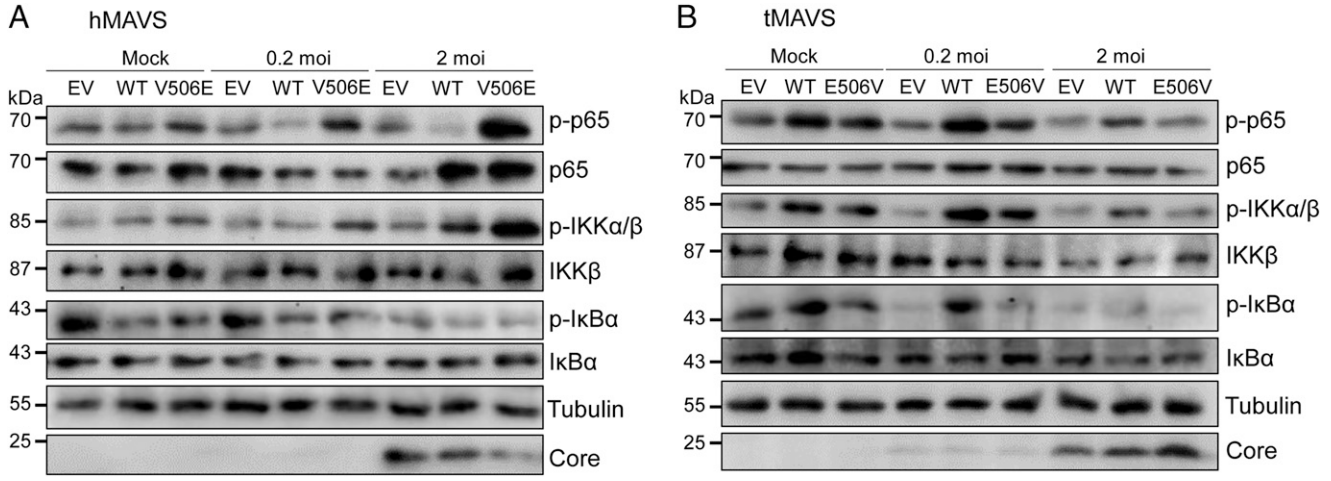

FIGURE 5. MAVS Glu^{506} affects the NF-κB signaling pathway. $Huh7.5.1^{MAVS\text{-}KO1}$ cells (4×10^5) were infected with HCV (MOI = 0.2 or 2) or uninfected (mock) for 72 h, then were transfected with (**A**) empty vector (EV) and expression vectors for hMAVS WT, hMAVS V506E, or (**B**) EV, tMAVS WT, or tMAVS E506V (2.5 μg each) for 48 h, respectively. Cell lysates were immunoblotted using the NF-κB signaling pathway sample kit. Shown are representative of three independent experiments, with similar results.

www.jimmunol.org/cgi/doi/10.4049/jimmunol.2001396

1 Table S1. Primers and vectors used in this study.

Primer	Sequence (5'-3') [a]	Restriction endonuclease	Application and vector
For Chinese tree shrew			
tMAVS F506 E→V	GAGGAGGAGCAGGAGGTGCCGTGTGTCAGGGTTTC		PCR to introduce a glutamate (E) to valine (V) mutation at the 506th residue in tMAVS using tMAVS-3Tag-6 vector
tMAVS R506 E→V	GAAACCCTGACACACGGCTCCTCCTGCTCCTCCTC		
tMAVS F508 C→R	AGCCATGAAACCCTGACACACGGCTCCTCCTGCTC		PCR to introduce a cysteine (C) to arginine (R) mutation at the 508th residue in tMAVS using tMAVS-3Tag-6 vector
tMAVS R508 C→R	AGCCATGAAACCCTGACACACGGCTCCTCCTGCTC		
tIKKβ 1F	CCC***AAGCTT***ATGAAAGAGCGACTGGGGAC	*Hin*d III	PCR for constructing tIKKβ expression vector (tIKKβ-3Tag-8) using pCMV-3Tag-8 vector
tIKKβ 2304R	CCG***CTCGAG***GGAGGCCCGCTCCAGGCTGT	*Xho* I	
tTRAF6 1F	CGC***GGATCC***ATGAGTCTGCTACACTGTGA	*Bam*H I	PCR for constructing tTRAF6 expression vector (tTRAF6-3Tag-8) using pCMV-3Tag-8 vector
tTRAF6 1617R	CCG***CTCGAG***TACCCCTGCATCAGTACTTC	*Xho* I	
tTRAF3 1F	CGC***GGATCC***ATGGAGTCGAGTAAAAAAAT	*Bam*H I	PCR for constructing tTRAF3 expression vector (tTRAF3-3Tag-8) using pCMV-3Tag-8 vector
tTRAF3 1566R	CCC***AAGCTT***GGGGTCGGGCAGGTCTGAAG	*Hin*d III	
tTBK1 1F	C***GAGCTC***ATGCAGAGCACTTCCAATCA	*Sac* I	PCR for constructing tTBK1 expression vector (tTBK1-3Tag-8) using pCMV-3Tag-8 vector
tTBK1 2187R	CCG***CTCGAG***AAGACAGTCCACGTTGCGAA	*Xho* I	
tMCP1 93F	TAGGACCTGCTGCTATGA		Analytical RT-qPCR (quantitative real-time PCR)
tMCP1 174R	ACAGTTGGTGTTCACTCTAC		
tIL8 F	GACAAGAATTGGTACAGAACT		Analytical RT-qPCR
tIL8 R	GGTCCACTCTCAATCACT		
For human			
MAVS-Sal-F	ACGC***GTCGAC***ATGCCGTTTGCTGAAGAC	*Sal* I	PCR for constructing hMAVS expression vector using pCMV-(DYKDDDDK)-C vector
MAVS-Bgl-R	GA***AGATCT***CTAGTGCAGACGCCGCCG	*Bgl* II	
hMAVS F508 C→R	GAGAGGGAGGTGCCACGCCACAGGCCCTCACCTG		PCR to introduce a cysteine (C) to arginine (R) mutation at the 508th residue in hMAVS using hMAVS expression vector
hMAVS R508 C→R	CCAGGTGAGGGCCTGTGGCATGGCACCTCCCTCTC		
hMAVS F506 V→E	CCAGGAGAGGGAGGAGCCATGCCACAGG		PCR to introduce a valine (V) to glutamate (E) mutation at the 506th residue in hMAVS using hMAVS expression vector
hMAVS F506 V→E	CCTGTGGCATGGCTCCTCCCTCTCCTGG		
hMAVS-sgRNA-F2	CACCGTCAGCCCTCTGACCTCCAGCG		For constructing CRISPR/Cas9 vector for hMAVS knockout using pX330-T7 vector
hMAVS-sgRNA-R2	AAACCGCTGGAGGTCAGAGGGCTGAC		
hMAVS-sgRNA-Fc	ATGCCTGTCCAGGAGACCC CTC		PCR for amplifying a region covering hMAVS sgRNA targeting sites
hMAVS-sgRNA-Rc	CACTTTGGAGGGCAGAGAG		
For HCV			
NS3/4A-F	CGC***GGATCC***GCTCCCATCACTGCTTATGC	*Bam*H I	PCR for constructing NS3/4A expression vector (Flag-NS3/4A) using pCMV-HA vector
NS3/4A-R	CCC***AAGCTT***GCATTCCTCCATCTCATCAA	*Hin*d III	

2 [a] Restriction endonuclease sites introduced by PCR are underlined and italicized.

Supplementary Figures

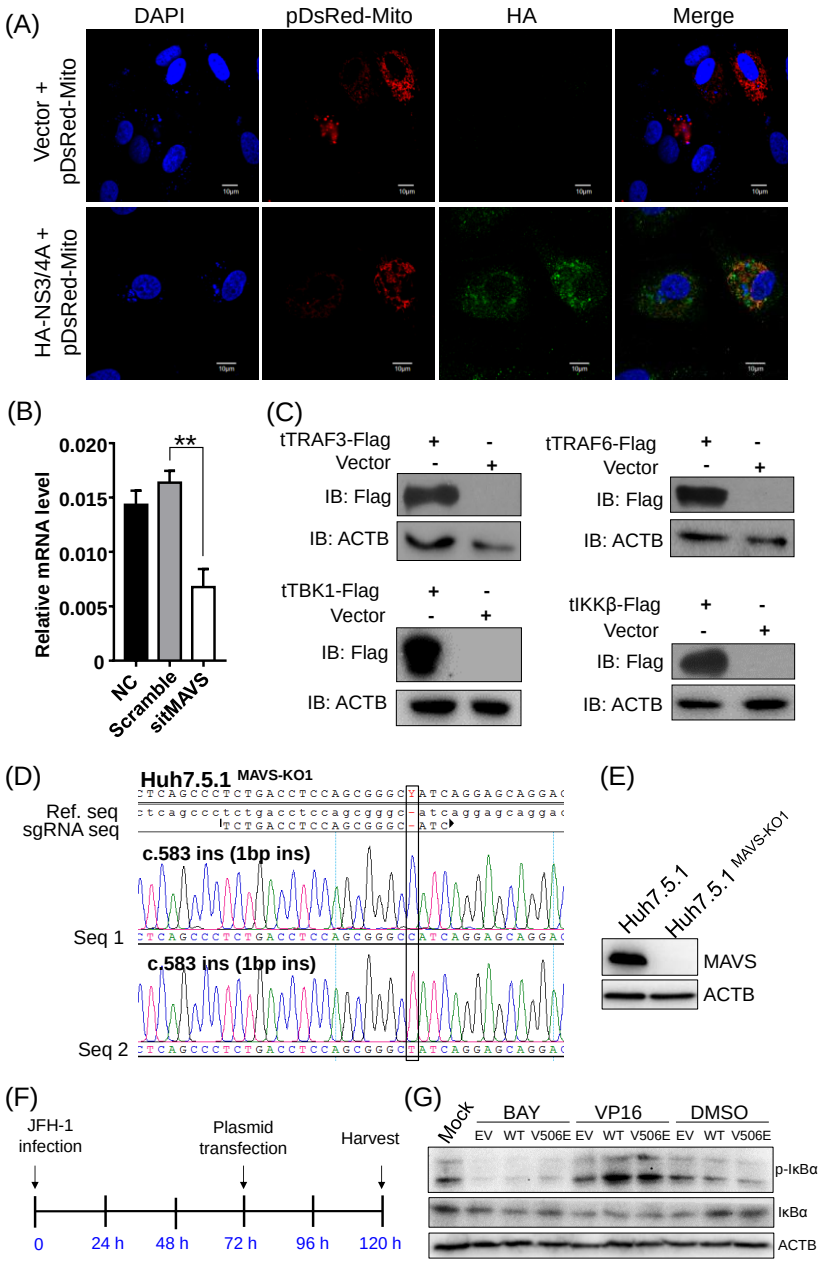

Figure S1. Characterization, quality control and experimental key materials.
(**A**) Alterations of mitochondrial structure when overexpression of the NS3/4A. Tree shrew primary renal cells (TSPRCs) were co-transfected with pDsRed-Mito and HCV NS3/4A-HA or empty vector (with a concentration ratio at 1:10) for 48 h. The localization of the NS3/4A protein was immunostained by using the anti-HA antibody and was visualized under a confocal microscopy. Nuclei were stained with DAPI. (**B**) Knockdown efficiency of *tMAVS* by using siRNA in primary tree shrew hepatocytes. Cells (1×10^6) were grown in 6-well plate overnight and were transfected with the indicated siRNA (sitMAVS or scramble, each 50 nM) or without transfection (NC) for 48 h before the harvest. The endogenous *tMAVS* mRNA level was analyzed by using quantitative real-time PCR. (**C**) Immunoblot analyses showing successful overexpression of tTRAF3, tTRAF6, tTBK1 or tIKKβ in TSPRCs. Cells (1×10^6) were transfected with the indicated expression vector or the empty vector (Vector, pCMV-3Tag-8 vector) for 48 h, then cells were harvested for immunoblot assays by using the anti-Flag and ACTB antibodies, respectively. (**D**) Sequencing chromatographs showing the introduced *hMAVS* mutations (c.583 insC or c. 583 insT) in Huh7.5.1 cells underwent gene editing (Huh7.5.1$^{\text{hMAVS-KO1}}$ cells). (**E**) Immunoblot analysis showing hMAVS knockout in Huh7.5.1$^{\text{MAVS-KO1}}$ cell line. (**F**) A schematic profile illustrating experimental design in the Huh7.5.1 $^{\text{hMAVS-KO1}}$ cells. (**G**) Effects of the NF-κB pathway inhibitor (BAY) and activator (VP16) treatment on the Huh7.5.1-hMAVS KO cells with or without MAVS rescue. Cells (1×10^6) were cultured in 6-well plates overnight, then were transfected with indicated vector (empty vector (EV) or expression vector for hMAVS WT or V506E, each 2.5 μg each) for 48 h, followed by treatment with BAY11 (10 μM), VP16 (10 μM) or DMSO (control) for 48 h. The ACTB was used as loading control for the immunoblot assay.
All data in (A-C, E and G) are representative of three independent experiments with similar results. ** $P < 0.01$, Student's *t* test. Bars represent mean ± SD of 3 biological repeats.